ELSEVIER

Cement & Concrete Composites 26 (2004) 323–330

Cement & Concrete Composites

www.elsevier.com/locate/cemconcomp

The hydration characteristics when C_2S is present in MSWI fly ash slag

K.S. Wang [a], K.L. Lin [b,*], T.Y. Lee [a], B.Y. Tzeng [a]

[a] Graduate Institute of Environmental Engineering, National Central University, Chung-Li 320, Taiwan, ROC
[b] Department of Environmental Engineering, National I-Lan Institute of Technology, I-Lan 260, Taiwan, ROC

Received 15 January 2002; accepted 5 July 2002

Abstract

This paper reports on an investigation of the hydration characteristics when C_2S is present in municipal solid waste incinerator (MSWI) slag. The results can be summarized as follows: thermogravimetric analysis (TGA) observations show lower amounts of CSH and $Ca(OH)_2$ in samples where C_2S is incorporated into MSWI slag, possibly due to the partial replacement (20–40%) of the mineral constituents by less active slag. In general, the incorporation of C_2S into slag, decreases the initial hydration reaction, whereas it increases the pozzolanic reactions at a later stage, by consuming $Ca(OH)_2$. The X-ray diffraction results are in good agreement with the TGA results. Moreover, the hydration degree of the C_2S–slag pastes, as determined by nuclear magnetic resonance techniques, also indicates that the C_2S–slag pastes show lower hydration degree values, at all ages (1–90 days) of hydration. This may be due to the inactive behavior of an acidic film on the grains of slag, which in term retards the hydration that occurs as the $Ca(OH)_2$ breaks down the silica framework.
© 2003 Elsevier Ltd. All rights reserved.

Keywords: MSW incinerator fly ash; Melting; Pozzolanic reactions; Nuclear magnetic resonance (NMR) techniques

1. Introduction

Due to its high heavy metal content, fly ash from the incineration of municipal solid waste is classified as hazardous waste in many countries, and must therefore be disposed of in specially designed landfills. More than 3000 metric tons of incinerated fly ash and bottom ash must be dealt with in Taiwan per day [1]. In general, these hazardous types of fly ash have to be detoxified, or stored in expensive secure landfills [2]. However, in response to a zero emissions goal, as part of a sustainable waste disposal solution, municipal solid waste incinerator (MSWI) fly ash that has been processed by melting, offers not only an alternative to detoxification, but also the possibility of it being recycled as construction material (mainly as fine aggregates) [3]. During the ash melting process, heavy metals and inorganic components in the ash are bound up molecularly into a glassy matrix [4], resulting in a chemically stable and physically durable product that is normally nontoxic in the natural environment [5]. However, in the alkaline environment of ordinary Portland cement, the fly-ash-derived slag becomes, in fact, chemically active, exhibiting self-cementing properties when pulverized and activated by the cement [6,7]. Thus, the use for melted MSWI fly ash to make slag blended cement could not only resolve both detoxification and disposal problems, but also provide the means to utilizing the recovered ash as construction material. Therefore, the physical property analyses, and a safety evaluation of the masonry units made from such ash-blended cement, must be provided and the hydraulic activity and the heavy metal leachability of the blends must be known.

Portland cement is a mixture with four principal constituents: $C_3S(Ca_3SiO_5)$ 50–70 wt.%; $C_2S(Ca_2SiO_4)$ 20–30 wt.%; $C_3A(Ca_3Al_2O_6)$ 5–12 wt.%; and $C_4AF(Ca_4Al_2Fe_2O_{10})$ 5–12 wt.% [8,9]. To gain better insight into the hydraulic characteristics of C_2S in MSWI slag, it is desirable to investigate the MSWI slag and its major compounds separately. There are very few publications concerning with the hydration of C_2S with MSWI slag, therefore, the present work is aimed at

* Corresponding author. Tel.: +886-3-422-7151x4660; fax: +886-3-422-1602.
E-mail address: kllin@mail.ev.ncu.edu.tw (K.L. Lin).

0958-9465/$ - see front matter © 2003 Elsevier Ltd. All rights reserved.
doi:10.1016/S0958-9465(02)00144-0

studying this. All the hydration products were investigated using thermogravimetric analysis (TGA) as well as X-ray diffraction (XRD) techniques, as well as nuclear magnetic resonance (NMR) techniques.

2. Materials and methods

2.1. Preparation of MSWI fly ash slag

The fly ash used in this study was collected from the cyclone of a mass-burning incinerator located in the northern part of Taiwan. The incinerator, capable of processing 1350 metric tons of local MSW per day, is equipped with air pollution control devices consisting of a cyclone, an adsorption reactor, and a fabric baghouse filter. The fly ash was homogenized, oven dried at 105 °C for 24 h, and then its chemical composition was characterized. The major components in the ash are shown in Table 1, with SiO_2, CaO, and Al_2O_3 comprising 16.8% (w/w), 10.6% (w/w), and 5.3% (w/w), respectively. The next most abundant components are Na_2O, K_2O, and Fe_2O_3, each contributing about 4.3% (w/w), 4.4% (w/w), and 3.5% (w/w), respectively. The ash has a basicity (defined as CaO/SiO_2) of 0.6, and a pouring point at approximately 1400 °C. The leaching concentrations, obtained by the toxic characteristic leaching procedure (TCLP) test, are presented in Table 2, showing the leachability of the heavy metals, Zn, Cr, and Cd.

The MSW fly ash slag was prepared by melting the above cyclone ash in a 20 l electric-heated melter at 1400 °C for 30 min. The melts were water-quenched to obtain fine slag, which was then ground in a ball mill until fine enough to pass through a #200 sieve. The resultant pulverized slag had a fineness of approximately 500 m^2/kg, with a specific gravity of 2.7.

Table 1
Chemical composition of β-C_2S, MSWI fly ash and slag

Composition	β-C_2S	MSWI fly ash	MSWI fly ash slag
CaO (%)	63.66	10.6	27.3
SiO_2 (%)	33.17	16.8	38.9
Al_2O_3 (%)	0.26	5.3	23.3
Fe_2O_3 (%)	0.06	3.5	5.4
MgO (%)	0.28	0.5	3.6
SO_3 (%)	<0.01	4.4	0.2
Na_2O (%)	<0.01	4.3	1.3
K_2O (%)	<0.01	4.4	<0.01
TiO_2 (%)	0.02	2.6	–
P_2O_5 (%)	0.01	1.1	–
Mn_2O_3 (%)	0.01	–	–
SrO (%)	0.05	–	–
Zn (mg/l)	–	7115	6480
Pb (mg/l)	–	1284	295
Cu (mg/l)	–	1409	604.4
Cr (mg/l)	–	811	695.3
Cd (mg/l)	–	80	5.8

*Construction Technology Laboratories, Inc., Skokie, IL, USA.

Table 2
TCLP leaching concentrations of heavy metals for MSWI fly ash and slag

Heavy metals	MSWI fly ash	Slag	Regulatory limits
Cd (mg/l)	1.8 ± 0.02	ND	1.0
Cr (mg/l)	4.3 ± 0.05	ND	5.0
Pb (mg/l)	0.7 ± 0.01	0.36 ± 0.02	5.0
Cu (mg/l)	0.6 ± 0.01	0.32 ± 0.05	–
Zn (mg/l)	16.2 ± 0.30	9.10 ± 0.33	–

Anhydrous β-C_2S was provided by the Construction Technology Laboratories, in Skokie, IL, USA. β-C_2S was used as the binding agent. The chemical compositions are listed in Table 1.

2.2. Paste tests

MSWI slag blended C_2S pastes (C_2S–slag) were produced by homogeneously mixing C_2S, pulverized slag, and water in a mixer. The mixture proportioning of the tested C_2S–slag pastes used a slag blend ratio ranging from 20% to 40%, with a constant water/binder (w/b) ratio of 0.38. C_2S–slag and C_2S paste cubes were prepared, according to ASTM C109, by pouring the paste into rectangular molds ($1 \times 1 \times 1$ in.), which stayed under ambient conditions for 24 h, then demolded, and cured in an environmental chamber, maintained at 25 °C with a relative humidity >98% for periods ranging from 1 to 90 days. Three specimens were used for compressive strength tests and the other one for microstructural examination. After curing for 1, 3, 7, 14, 28, 60 or 90 days, the C_2S–slag and C_2S paste cubes were subjected to unconfined compressive strength (UCS) tests. An average strength from the three specimens is presented. Subsequently, the crushed samples, whose hydration reactions were terminated with methyl alcohol for 24 h. They were then subjected to XRD, TGA, and ^{29}Si MAS/NMR (^{29}Si nuclear magnetic resonance) analyses.

2.3. Analytical methodology

The major analyses performed on the C_2S–slag pastes and its cubes included TCLP, and chemical composition determination as follows:

- TCLP: SW 846-1311.
- Chemical composition: Inductively coupled plasma-atomic emission spectrometer.
- Leaching concentration: Cd (SW846-7131A), Pb (SW846-7421), Zn (SW846-7951), Cu (SW846-7211), Cr (SW846-7191).
- XRD: The XRD analyses were carried out by a Siemens D-5000 X-ray diffractometer with Cu Kα radia-

tion and 2Θ scanning, ranging between 5° and 70°. The XRD scans were run at 0.05° steps, with a 1 s counting time.

- TGA: TGA analyses of the samples were performed using a Seiko SSC Model 5000 thermal analyzer. Dry N_2 gas was used as a stripping gas and a heating rate of 0.5 °C/min was used. The samples were heated from 25 to 1007 °C.
- Chemical shift of linear polysilicate anions in calcium silicate hydrate (C-S-H):^{29}Si nuclear magnetic resonance (^{29}Si MAS/NMR).

The degree of hydration of the cement clinkers, both C_2S and C_3S, and the average length of linear polysilicate anions in the C-S-H gels, primarily responsible for the strength, were analyzed by using high resolution solid state ^{29}Si MAS/NMR techniques as follows:

The increase of diamagnetic shielding to the ^{29}Si nuclei that resulted from the degree of increasing condensation from the single tetrahedral structure of the monosilicates (Q^0) to the end groups (Q^1), to the chain middle groups (Q^2), to the layers and branching sites (Q^3), and finally to the three-dimensional frameworks (Q^4), led to well-separated and analytically useful chemical shift ranges for each type of SiO_4 unit [10,11]. That is, the C-S-H's, the hydration products in the cement, could be semi-quantified using chemical shifts in the ^{29}Si nuclei in the Si–O–X groups, for which the structures are shown below [12]:

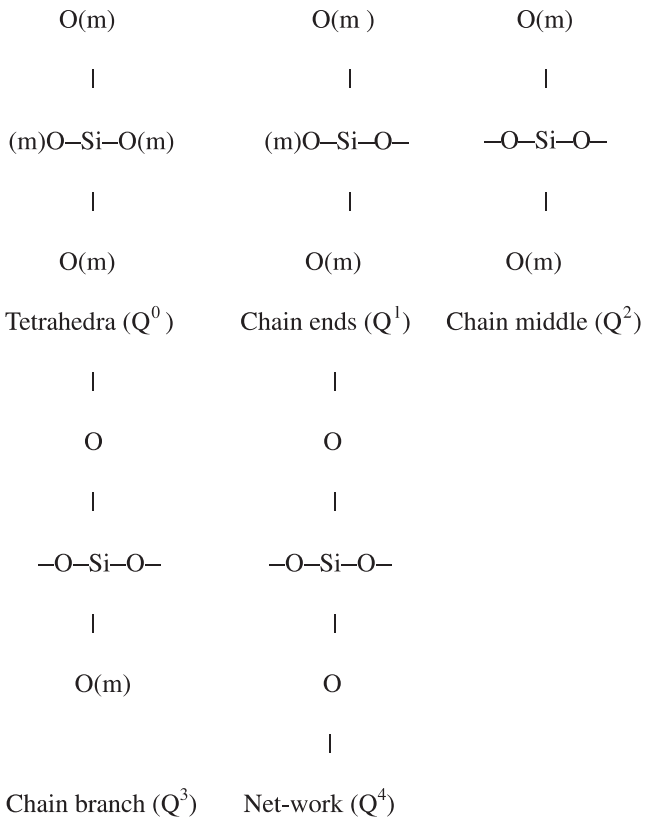

Table 3
Range of ^{29}Si chemical shifts of Q^n units in solid silicates

Types of Si–O–X group	Symbol	Range (ppm)
Monosilicates	Q^0	−68 to −76
Disilicates and chain end group	Q^1	−76 to −82
Chain middle groups	Q^2	−82 to −88
Chain branching sites	Q^3	−88 to −92
Three-dimensional framework	Q^4	−92 to −129

High-resolution ^{29}Si MAS/NMR spectra were recorded at 39.72 MHz on an MSL Bruker MAS/NMR-200 solid-state high-resolution spectrometer, using rapid (about 3 kHz) sample spinning at the magic angle to the external magnetic field. The ^{29}Si chemical shifts are given relative to the primary standard liquid tetramethylsilane in the delta-scale (the negative signs correspond to up-field shifts). The sharp ^{29}Si signal chemical shifts for the above Si–O–X groups in solid silicates are summarized in Table 3.

The hydration degree (designated as α of the cement clinkers, both C_2S and C_3S, can be evaluated as follows by the integral intensity of the signals at −70 ppm (Q^0) for both the hydrated cement paste and cement powders, i.e., $I^0(Q^0)$ and $I(Q^0)$, respectively:

$$\alpha = \left[1 - \frac{I(Q^0)}{I^0(Q^0)}\right] \times 100\%. \quad (1)$$

3. Results and discussion

3.1. Characterization of MSWI Fly Ash and Slag

Table 1 lists the major components of the MSWI slag used in this study. The slag was composed of SiO_2 (38.9% w/w), CaO (27.3% w/w), and Al_2O_3 (23.3% w/w). The furnace outlet temperature was about 1400 °C. Cd, Zn, Cr and Pb, whose boiling points (or sublimation point) are lower than this temperature, evaporated and became trapped in the exhaust gas treatment system, so the slag fixed ratios of these metals were low. High vapor pressure metals such as Cd, Pb, and Zn are difficult to retain in the melt and slag with which they

Table 4
UCS of C_2S and C_2S–slag paste samples for different curing times

Curing time (day)	Compressive strength (MPa)		
	100% C_2S	80% C_2S + 20% slag	60% C_2S + 40% slag
1	1	1	1
3	1	1	1
7	3	2	1
28	9	3	1
60	28	5	1
90	32	5	1

evaporate during high-temperature melting process. On the other hand, Cu, which has higher boiling points than the furnace outlet temperature, moved into the slag.

The resultant slags were analyzed for leachability characteristics using the TCLP analysis. Melting processing was found to increase the leach-resistance of the slag. Therefore, the TCLP leaching concentrations of the heavy metals all met the EPA's current regulatory thresholds.

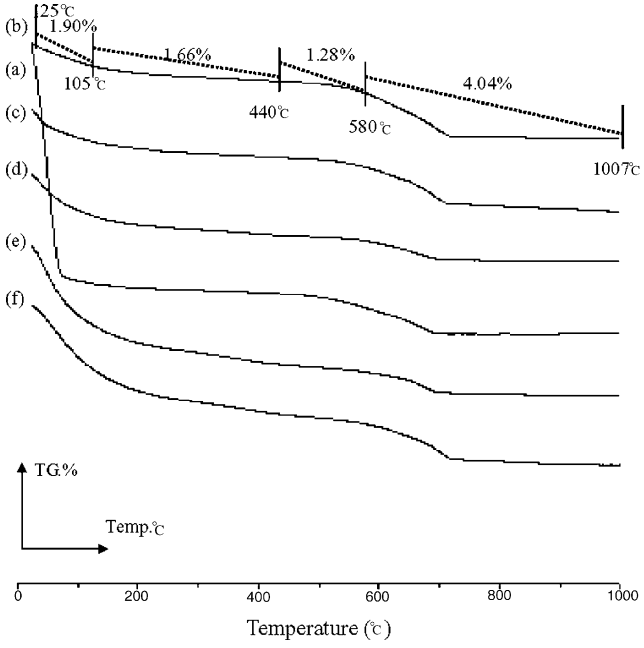

Fig. 1. TGA of hydrated C_2S pastes for different curing times (a) 1 day; (b) 3 days; (c) 7 days; (d) 28 days; (e) 60 days; (f) 90 days.

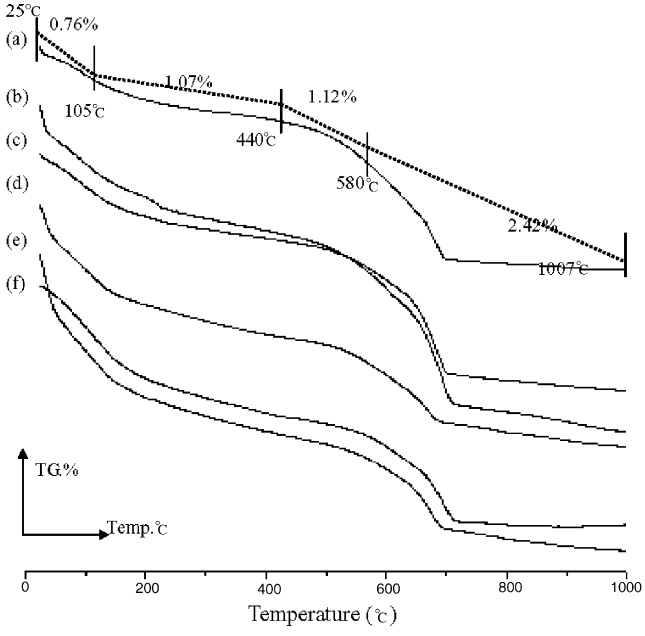

Fig. 2. TGA of hydrated C_2S–slag pastes (replacement ratio = 20%) for different curing times (a) 1 day; (b) 3 days; (c) 7 days; (d) 28 days; (e) 60 days; (f) 90 days.

3.2. Development of unconfined compressive strength

Table 4 exhibits the development of the UCS in the C_2S–slag and C_2S paste monoliths with the curing time.

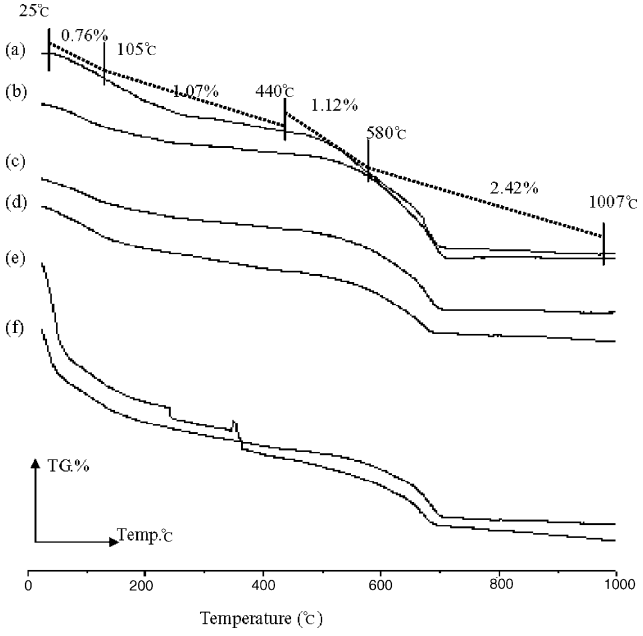

Fig. 3. TGA of hydrated C_2S–slag pastes (replacement ratio = 40%) for different curing times (a) 1 day; (b) 3 days; (c) 7 days; (d) 28 days; (e) 60 days; (f) 90 days.

Table 5
Mass loss during the TG analysis of pure C_2S and C_2S–slag pastes

Samples	Curing time (day)	Weight loss (%)			
		H_2O	CSH	$Ca(OH)_2$	$CaCO_3$
100% C_2S	1	21.92	1.17	1.44	2.13
	3	1.90	1.66	1.28	4.04
	7	2.78	1.67	1.00	4.03
	28	3.66	2.04	0.86	1.67
	60	7.03	3.98	0.87	2.01
	90	5.73	4.45	0.79	3.63
80% C_2S+ 20% slag	1	0.76	1.07	1.12	2.42
	3	1.45	1.69	0.98	3.79
	7	0.84	1.27	0.70	2.91
	28	1.54	1.66	0.67	1.96
	60	2.45	1.95	0.64	2.11
	90	1.23	1.98	0.54	2.05
60% C_2S+ 40% slag	1	0.73	1.02	1.02	2.30
	3	0.57	0.93	0.74	2.41
	7	0.57	0.96	0.62	1.89
	28	0.64	1.31	0.56	1.55
	60	3.32	1.51	0.68	1.79
	90	2.10	1.53	0.48	1.75

It is noted that the UCS at all stage (1–90 days) showed a decrease with an increase in the slag replacement.

3.3. Thermogravimetric analysis of C_2S and C_2S–slag pastes

The hydration products of both pure and C_2S–slag pastes, were cured up to 90 days, followed by a TGA, which is shown in Figs. 1–3. Fig. 1 gives the TGA for C_2S pastes, which show four endothermic effects, at 25–105, 105–440, 440–580 and 580–1007 °C. The first mass loss in the C_2S samples occurred at 25–105 °C, related to adsorbed moisture. Mackenzie [13] reported a mass loss for C-S-H, due to dehydration reactions, at 105–440 °C. The third peak can be attributed to the decomposition of $Ca(OH)_2$. The higher temperature endothermic effect, over 580 °C is due to the decomposition of $CaCO_3$ with a different crystallinity. CSH reacts with CO_2 or CO_3^{2-} ion with formation of $CaCO_3$ [14]. Table 4 indicates that as the hydration proceeds, the amount of CSH increases. It can be seen that pure C_2S hydrates slowly by producing CSH, which increases over time.

Fig. 2 which shows the TGA of C_2S with 20% slag pastes, also illustrates endothermic effects, at 25–105, 105–440, 440–580 and 580–1007 °C. On the other hand, $Ca(OH)_2$ is formed in smaller amounts than for C_2S pastes. As the hydration process proceeds, the amount of CSH gel, at 400–450 °C, increases with time. Table 5 indicates that the C_2S slag pastes have lower CSH values than the pure C_2S pastes, at all stages of hydration. This may be due to the retarding effect of $Ca(OH)_2$, which

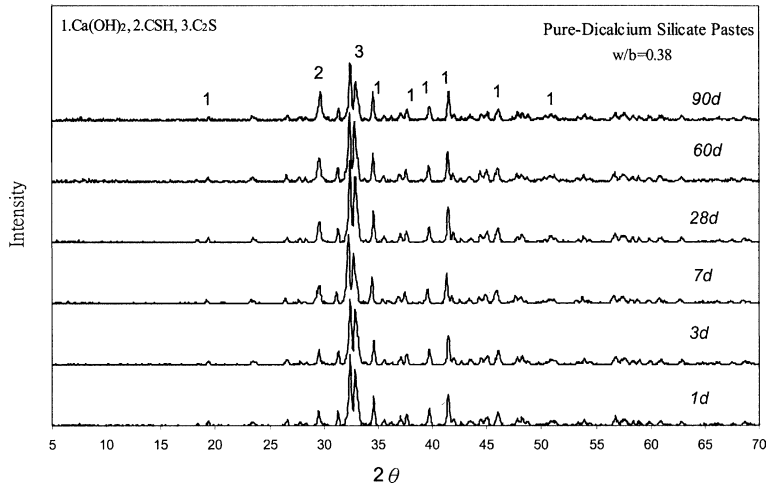

Fig. 4. XRD patterns of hydrated C_2S pastes.

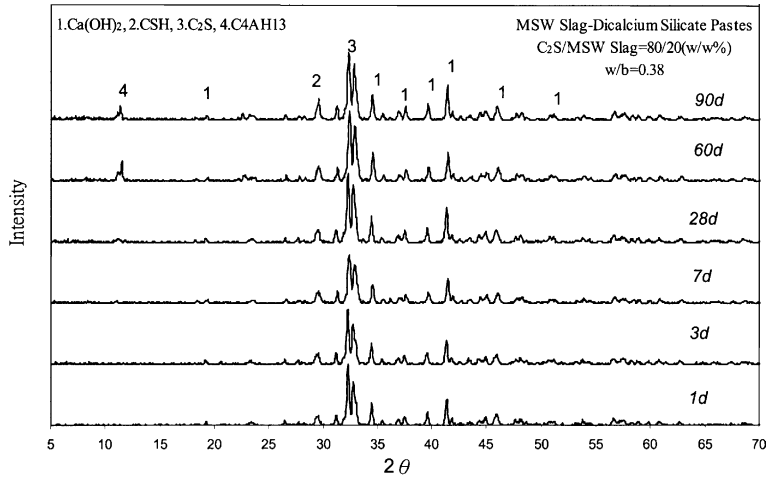

Fig. 5. XRD patterns of hydrated C_2S with 20% slag pastes.

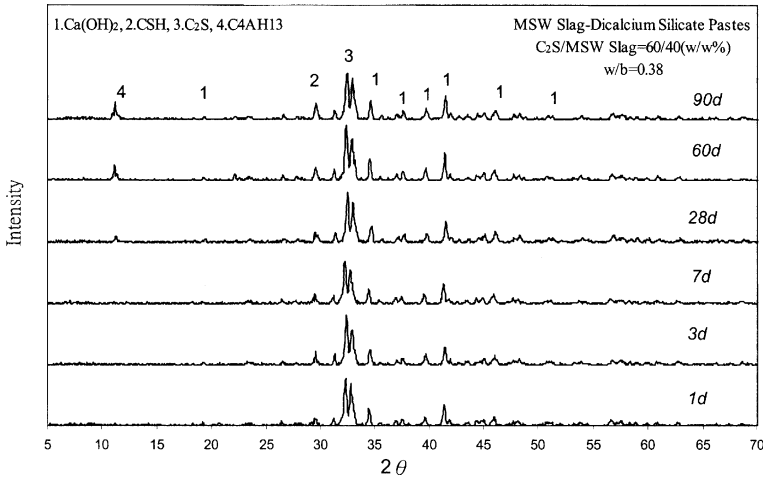

Fig. 6. XRD patterns of hydrated C_2S with 40% slag pastes.

coats the C_2S grains. Therefore, the pulverized slag is a latent hydraulic material.

3.4. Changes of hydration products in the C_2S and C_2S–slag pastes

The XRD patterns for the hydration products of pure C_2S and C_2S–slag pastes, and the curing times, can be seen in Figs. 4–6. Fig. 4 indicates the XRD patterns of hydrated C_2S pastes, it is clear that the CSH increases up to 90 days.

Figs. 5 and 6 shows the XRD patterns of hydrated C_2S–slag paste samples, indicating the CSH, C_4AH_{13} and residual C_2S peaks. As the hydration proceedes, the C_4AH_{13} peaks can be clearly seen after 28 days. The CSH peaks increase, up to 90 days, due to the activation of the slag by liberated $Ca(OH)_2$. The XRD results are in good agreement with the TGA results.

3.5. NMR analysis of C_2S and C_2S–slag pastes

Figs. 7–9 present the ^{29}Si MAS/NMR spectra of the hydrated samples of pure C_2S and C_2S–slag pastes, at various stages. These and the other results are summarized in Table 6. Table 6 shows the increased intensity of signals from Q^2 silicon sites in the hydrated, mechanically activated blends. It is known that the CSH, formed by the hydration of calcium silicates, is generally dominated by Q^1 sites, or has abundant Q^1 and Q^2 sites. The ratio, Q^2/Q^1 of silicon sites in the hydrated products, also rises after the mechanical activation of the blends. The hypothesis that in MSWI slag thin SiO_2 layers form around C_2S crystals, which accelerates the pozzolanic reaction and promotes the growth of more extensive nets of hydrated products, is suggested.

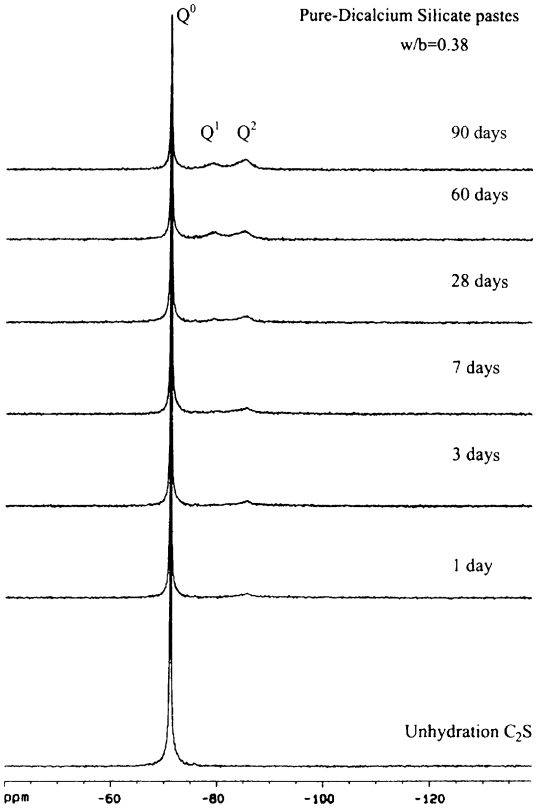

Fig. 7. ^{29}Si MAS/NMR spectra of hydrated C_2S pastes.

Table 6 indicates the hydration degree of pure C_2S, as well as the C_2S–slag pastes, up to 90 days. It is seen that the hydration degree of pure C_2S increases with time. Also, the C_2S–slag pastes show lower hydration degree values at all ages of hydration. This may be due to the sluggish behavior of slag formation due to an acidic film on the grains of slag, that retards the hydration process, which occurs as the $Ca(OH)_2$ breaks down the silica

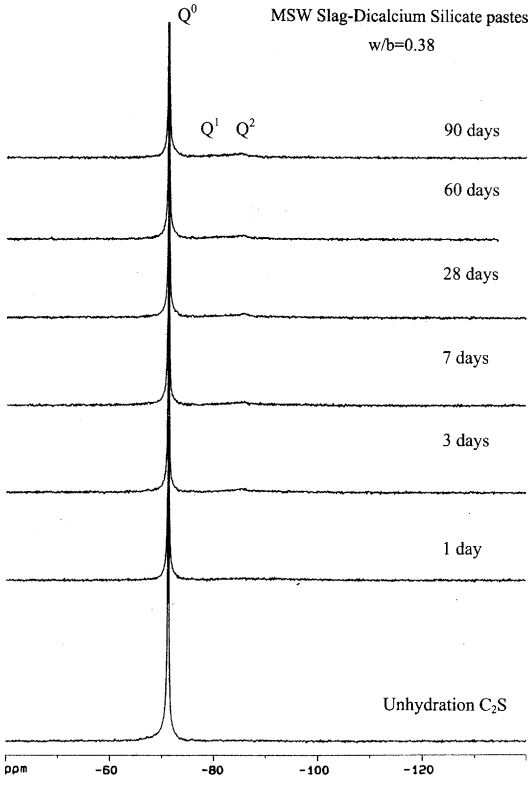

Fig. 8. ^{29}Si MAS/NMR spectra of hydrated C_2S with 20% slag pastes.

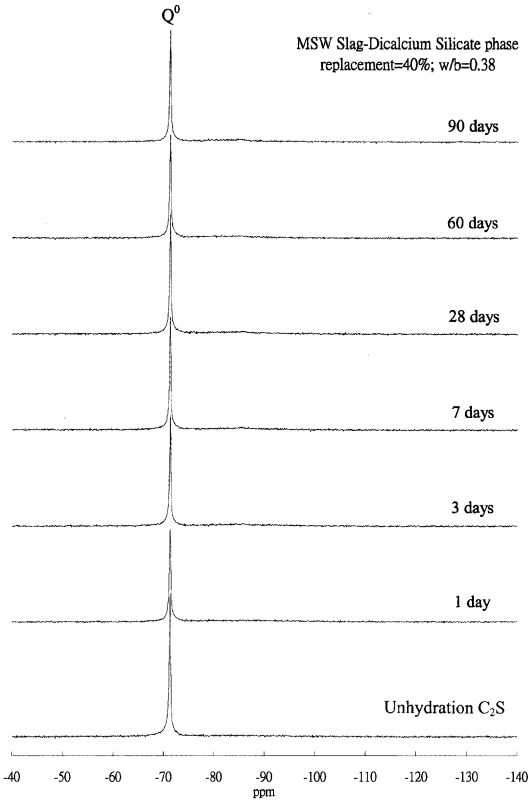

Fig. 9. ^{29}Si MAS/NMR spectra of hydrated C_2S with 40% slag pastes.

Table 6
^{29}Si NMR analysis for slag blended monoliths and different curing times

Samples	Curing time (day)	^{29}Si NMR integral intensities of Q^n						α (%)
		Q^0	Q^1	Q^2	Q^3	Q^4	Total	
100% C_2S	Unhydrated	951	0	0	0	49	1000	
	1	832	20	96	24	27	1000	12.5
	3	825	27	96	24	29	1000	13.3
	7	766	58	118	17	40	1000	19.4
	28	756	79	143	12	10	1000	20.4
	60	659	157	173	2	8	1000	30.7
	90	600	149	226	5	20	1000	37.0
80% C_2S + 20% slag	Unhydrated	935	9	9	3	44	1000	
	1	810	31	59	32	69	1000	13.4
	3	809	31	89	29	42	1000	13.5
	7	812	34	89	24	40	1000	13.1
	28	808	48	95	23	26	1000	13.6
	60	808	59	100	12	21	1000	13.6
	90	803	64	102	11	19	1000	14.1
60% C_2S + 40% slag	Unhydrated	917	10	10	3	60	1000	
	1	829	29	83	18	41	1000	9.6
	3	815	32	80	31	43	1000	11.1
	7	814	35	87	24	40	1000	11.2
	28	809	48	94	23	26	1000	11.7
	60	806	62	94	21	18	1000	12.1
	90	803	64	102	11	19	1000	12.4

framework of the slag. It was formerly believed that some combination occurred between $Ca(OH)_2$ and the slag but at later ages a progressive take-up of $Ca(OH)_2$ forming hydrated compounds [14].

4. Conclusions

This study investigates the hydration characteristics when C_2S is present in MSWI slag. They can be summarized as follows:

1. Lower CSH and $Ca(OH)_2$ amounts in C_2S samples incorporated in MSWI slag were observed, possibly due to the partial replacement of the mineral constituents by less active slag.
2. The incorporation of C_2S into slag decreases the initial hydration reaction, whereas it increases the pozzolanic reaction at a later stage, by consuming $Ca(OH)_2$ to form CSH.
3. The XRD results are in good agreement with the DTA results.
4. ^{29}Si MAS/NMR techniques indicate that C_2S–slag pastes show a lower degree of hydration for all hydration ages. This may be due to the sluggish behavior of slag formation by an acidic film on the grains of slag, retarding hydration process, which occurs as the $Ca(OH)_2$ breaks down the silica framework.

References

[1] Yang WF. Report of Department of Environmental Protection. Taipei Municipal Government, ROC EPA, 1999.
[2] Pera J, Wolde A, Michel C. Hydraulic activity of slags obtained by vitrification of wastes. ACI Mat J 1996;93(M70): 613–8.
[3] Bhatty JI, Reid KJ. Compressive strength of sludge ash mortars. ACI Mat J 1989;86(M34):394–400.
[4] Abe SI, Kambayashi F, Okada M. Ash melting treatment by rotating type surface melting furnace. Waste Manage 1996;16: 431–43.
[5] Mindess S, Young JF. Concrete. NJ: Prentice-Hall Inc; 1981.
[6] Mehta PK. Concrete. NJ: Prentice-Hall Inc; 1986.
[7] Roy DM, Idorn GM. Hydration structure and properties of blast furnace slag cements. ACI Mat J 1982;79:444–57.
[8] Freidin C. Hydration and strength development of binder based on high-calcium oil shale fly ash. Cement Concrete Res 1998;28: 829–39.
[9] Lin CK, Chen JN, Lin CC. An NMR, XRD and EDS study of solidification/stabilization of chromium with Portland cement and C_3S. J Hazardous Mat 1997;56:21–34.
[10] Hjorth J. The ^{29}Si MAS/NMR studies of Portland cement components and effects of microsilica on the hydration reaction. Cement Concrete Res 1988;18:788–98.
[11] Engelhardt G, Michel D. High-resolution solid-state NMR of silicates and zeolites. NY: John Wiley & Sons; 1987.
[12] Tustnes H, Bjoergum IM, Krane J, Skjetne T. NMR—A powerful tool in cement and concrete research. Adv Cement Res 1990;30(11):105–13.
[13] Mackenzie RC. Differential thermal analysis. NY: Academic Press; 1970.
[14] Taylor HFW. Cement chemistry. NY: Academic Press; 1990.